J|A|C|S
ARTICLES
Published on Web 06/30/2006

Substituent Effects in the Hydrosilylation of Coordinated Dinitrogen in a Ditantalum Complex: Cleavage and Functionalization of N_2

Bruce A. MacKay, Rui F. Munha, and Michael D. Fryzuk*

Contribution from the Department of Chemistry, The University of British Columbia, 2036 Main Mall, Vancouver, British Columbia, Canada V6T 1Z1

Received March 3, 2006; E-mail: fryzuk@chem.ubc.ca

Abstract: The dinitrogen complex ([NPN]Ta)$_2$(μ-η^1:η^2-N$_2$)(μ-H)$_2$, **1**, (where [NPN] = (PhNSiMe$_2$CH$_2$)$_2$PPh) undergoes hydrosilylation with primary and secondary alkyl- and arylsilanes, giving a new N−Si bond and a new terminal tantalum hydride derived from one Si−H unit. Various primary silanes can be employed to give isolable complexes of the general formula ([NPN]TaH)(μ-N−N−SiH$_n$R$_{3-n}$)(μ-H)$_2$(Ta[NPN]) (**5**, R═Bu, n = 2; **9**, R═Ph, n = 2). Analogous complexes featuring secondary silanes are not isolable, because these products, and **5** and **9**, are uniformly unstable toward reductive elimination of bridging hydrides as H$_2$, followed by cleavage of the N−N bond to give ([NPN]TaH)(μ-N)(μ-N−SiH$_n$R$_{3-n}$)(Ta[NPN]) (**6**, R═Bu, n = 2; **10**, R═Ph, n = 2; **15**, R═Ph, n = 1; **16**, R═Ph and Me, n = 1). The bridging nitrido ligand in these complexes is itself a substrate for a second hydrosilylation when n = 2, and schemes leading to Ta(IV) complexes of the general formula ([NPN]Ta)$_2$(μ-N−SiH$_2$R)(μ-N−SiH$_2$R') via elimination of H$_2$ are reported (**4**, R═R′ = Bu; **12**, R═Bu, R′ = Ph; **13**, R═Bu, R′ = CH$_2$CH$_2$SiH$_3$). At this point, the general reaction manifold for these compounds ramifies, with distinct outcomes occurring for different R groups—[NPN] ligand amide migration from Ta to RSi affords **11**, ([NPN]Ta(μ-NSiH$_2$Ph)(μ-NSiH$_2$Ph)Ta[NPN]), whereas stable complex **6** rearranges to give **7**, ([NP(C$_6$H$_4$)N]Ta(BuSiH$_2$N-μ-SiHBu-μ-N)Ta[NPN]) in the presence of excess silane. Ethanediylbissilane reacts with **1** to give **14**, ([NP(C$_6$H$_4$)N]Ta(N−SiH$_2$CH$_2$CH$_2$Si(H)-μ-N)Ta[NPN]), isostructural to **7**.

Introduction

Activation of molecular nitrogen by soluble metal complexes has historically been concerned with the synthesis of new dinitrogen-containing compounds.[1−3] As a result of this extensive early work, much is known about different bonding modes for the N_2 molecule and general synthetic methods for the preparation of dinitrogen complexes.[4] But what has lagged behind is the development of reactivity patterns that result in functionalization at bound N_2 and/or N−N bond cleavage. Such fundamental processes that involve transformation of the dinitrogen unit are key to the direct utilization of molecular nitrogen as a reagent in the formation of higher-value organonitrogen materials.[5]

Despite the fact that there are hundreds of N_2 complexes known, there are only a handful of these derivatives that undergo further reactivity at the N_2 unit.[6,7] Protonation of coordinated dinitrogen has been used extensively in stoichiometric processes involving group 6 complexes that result in further elaboration of the dinitrogen unit,[8,9] and there is one example of a system that can be made to turnover to generate more than stoichiometric quantities of NH_3 with judicious choice of acid and reducing agent.[10,11] Reaction of coordinated N_2 with various electrophiles has been well studied and used to generate a variety of new kinds of bonds N−X bonds.[12−18] More recently, certain zirconium[19−22] and hafnium[23] dinitrogen complexes have been

(1) Chatt, J.; Dilworth, J. R.; Richards, R. L. *Chem. Rev.* **1978**, *78*, 589.
(2) Gambarotta, S. *J. Organomet. Chem.* **1995**, *500*, 117.
(3) Hidai, M. M. Y. *Chem. Rev.* **1995**, *95*, 1115.
(4) Fryzuk, M. D.; Johnson, S. A. *Coord. Chem. Rev.* **2000**, *200−202*, 379.
(5) Fryzuk, M. D. *Chem. Rec.* **2003**, *3*, 2.
(6) Shaver, M. P.; Fryzuk, M. D. *Adv. Synth. Catal.* **2003**, *345*, 1061.
(7) MacKay, B. A.; Fryzuk, M. D. *Chem. Rev.* **2004**, *104*, 385.
(8) Hidai, M.; Mizobe, Y. *Can. J. Chem.* **2005**, *83*, 358.
(9) Hidai, M. *Coord. Chem. Rev.* **1999**, *185−186*, 99.
(10) Yandulov, D. V.; Schrock, R. R. *Science* **2003**, *301*, 76.
(11) Ritleng, V.; Yandulov, D. V.; Weare, W. W.; Schrock, R. R.; Hock, A. S.; Davis, W. M. *J. Am. Chem. Soc.* **2004**, *126*, 6150.
(12) Figueroa, J. S.; Piro, N. A.; Clough, C. R.; Cummins, C. C. *J. Am. Chem. Soc.* **2006**, *128*, 940.
(13) Betley, T. A.; Peters, J. C. *J. Am. Chem. Soc.* **2003**, *125*, 10782.
(14) Greco, G. E.; Schrock, R. R. *Inorg. Chem.* **2001**, *40*, 3861.
(15) Leigh, G. J. *Acc. Chem. Res.* **1992**, *25*, 177.
(16) O'Donoghue, M. B.; Davis, W. M.; Schrock, R. R. *Inorg. Chem.* **1998**, *37*, 5149.
(17) O'Donoghue, M. B.; Davis, W. M.; Schrock, R. R.; Reiff, W. M. *Inorg. Chem.* **1999**, *38*, 243.
(18) O'Donoghue, M. B.; Zanetti, N. C.; Davis, W. M.; Schrock, R. R. *J. Am. Chem. Soc.* **1997**, *119*, 2753.
(19) Pool, J. A.; Lobkovsky, E.; Chirik, P. J. *Nature* **2004**, *427*, 527.
(20) Fryzuk, M. D.; Love, J. B.; Rettig, S. J.; Young, V. G. *Science* **1997**, *275*, 1445.
(21) Basch, H.; Musaev, D. G.; Morokuma, K.; Fryzuk, M. D.; Love, J. B.; Seidel, W. W.; Albinati, A.; Koetzle, T. F.; Klooster, W. T.; Mason, S. A.; Eckert, J. *J. Am. Chem. Soc.* **1999**, *121*, 523.
(22) Bernskoetter, W. H.; Lobkovsky, E.; Chirik, P. J. *J. Am. Chem. Soc.* **2005**, *127*, 14051.

10.1021/ja061508q CCC: $33.50

found to react with H_2 and silanes to generate new species with N−H and N−Si bonds;[20] these latter examples are important as they involve functionalization of N_2 via reaction with reagents that have relatively nonpolar bonds. The reaction of terminal alkynes can also result in functionalization of the dinitrogen moiety to form either N−C bonds[24] or N−H bonds,[25] depending on the ancillary ligand system utilized. Reductive cleavage of the dinitrogen moiety has been examined with some group 5 and 6 metal complexes;[26−30] in a few of these systems, intermediates have been observed that have shed light on important mechanistic issues.

One of the more versatile dinitrogen complexes that shows a remarkable breadth of reactivity patterns is the ditantalum complex ([NPN]Ta)$_2$(μ-η^1:η^2-N_2)(μ-H)$_2$, **1**.[31] The unique side-

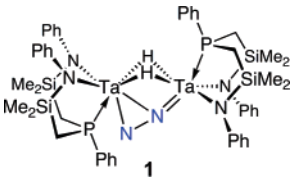

1

on end-on bonding mode for the N_2 moiety in this complex[32] has been examined, and its Lewis basicity[33] can be attributed to the existence of a "lone pair" on the exposed terminal nitrogen atom in the molecular HOMO-1. In addition, there is pronounced π character to the Ta−N bonding in the HOMO.[34,35] Although this complex undergoes reaction with electrophiles such as benzyl bromide to generate the expected N−C bond of the benzyl-hydrazido unit in ([NPN]TaBr)(μ-H)$_2$(μ-η^1:η^2-NNCH$_2$Ph)(Ta[NPN]),[31] a more important reaction is the addition of simple main-group hydrides of the general formula E−H to the starting N_2 complex **1**. For example, when E−H is 9-borabicyclo[3.3.1]nonane (9-BBN), the Ta−N π bond is hydroborated[34] to generate ([NPN]TaH)(μ-H)$_2$(μ-η^1:η^2-NNBC$_8$H$_{11}$)(Ta[NPN]), **2**, in which the N_2 unit is functionalized with concomitant formation of a new tantalum hydride. This reaction is general and proceeds identically for both primary and secondary boranes.[35] Remarkably, this simple adduct **2** is unstable and undergoes a cascade of events that include reductive elimination of the bridging hydride ligands as H_2 and eventual ancillary ligand degradation to ultimately generate modest yields of imide-nitride derivatives.

Extension of this E−H addition chemistry to hydroalumination of **1**[36] follows a similar reaction course, at least initially. Reaction of **1** with diisobutylaluminum hydride (DIBAL-H) at low temperatures results in the formation of the analogous organoaluminum adduct ([NPN]TaH)(μ-H)$_2$(μ-η^1:η^2-NNAlBu$^i_2$)(Ta[NPN]), **3**; however, in this case, further rearrangement involves [NPN] ligand amide migration from Ta to Al and elimination of isobutene to generate a species with a nitride bridging between Al and Ta.

In both hydroboration and hydroalumination, N−N bond cleavage is observed after functionalization at nitrogen. In fact, prior E−H addition to form N−B and N−Al bonds and the terminal Ta−H bond in **2** and **3**, respectively, is necessary to promote loss of H_2, which in turn provides the necessary two electrons needed to cleave the N−N bond.

We have previously communicated[37] the preliminary results of our study into the hydrosilylation reaction (E−H = BuSiH$_3$) of dinitrogen complex **1**. Although this example of E−H addition shares some common features with both hydroboration and hydroalumination, there are some intriguing differences for the hydrosilylation process, which include substituent effects, access to key intermediates, and isolation of different kinds of products. In this work, we provide full details of the reaction of primary, secondary, and tertiary silanes with **1**.

Results and Discussion

Hydrosilylation Using Butylsilane (BuSiH$_3$). When dinitrogen complex **1** is allowed to react with slightly more than 2 equiv of butylsilane (BuSiH$_3$), the dinuclear disilylimide **4** can be isolated as a crystalline red solid in good yields (eq 1).[37] The solution NMR data indicate a highly symmetric structure for **4**, which was confirmed by the solid-state X-ray crystal structure, as previously reported.

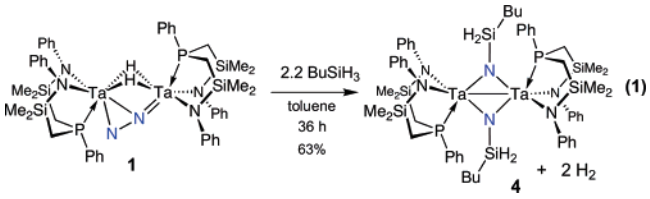

As compared to the aforementioned hydroboration and hydroalumination reactions, wherein considerable ligand rearrangement accompanies functionalization and N−N bond cleavage, the hydrosilylation process is certainly more straightforward and potentially more useful because both nitrogen atoms have been silylated, despite their asymmetric activation in **1**.

Upon monitoring the reaction of **1** with butylsilane using ^{31}P NMR spectroscopy, a number of intermediates were observed to grow as a function of time. In fact, two of these intermediates could be isolated by controlling stoichiometry, temperature, and reaction times. Also evident by this experiment was the eventual transformation of the intermediates to disilylimide **4**, and under certain conditions, the disilylimide itself undergoes a further reaction. All of these processes are quite amenable to study using ^{31}P NMR spectroscopy because each complex observed features unique and characteristic chemical shifts and, in some cases, J_{PP} coupling constants. We have previously explored the

(23) Bernskoetter, W. H.; Olmos, A. V.; Lobkovsky, E.; Chirik, P. J. *Organometallics* **2006**, *25*, 1021.
(24) Morello, L.; Love, J. B.; Patrick, B. O.; Fryzuk, M. D. *J. Am. Chem. Soc.* **2004**, *126*, 9480.
(25) Bernskoetter, W. H.; Pool, J. A.; Lobkovsky, E.; Chirik, P. J. *J. Am. Chem. Soc.* **2005**, *127*, 7901.
(26) Kawaguchi, H.; Matsuo, T. *Angew. Chem., Int. Ed.* **2002**, *41*, 2792.
(27) Laplaza, C. E.; Cummins, C. C. *Science* **1995**, *268*, 861.
(28) Laplaza, C. E.; Johnson, M. J. A.; Peters, J. C.; Odom, A. L.; Kim, E.; Cummins, C. C.; George, G. N.; Pickering, I. J. *J. Am. Chem. Soc.* **1996**, *118*, 8623.
(29) Clentsmith, G. K. B.; Bates, V. M. E.; Hitchcock, P. B.; Cloke, F. G. N. *J. Am. Chem. Soc.* **1999**, *121*, 10444.
(30) Mindiola, D. J.; Meyer, K.; Cherry, J.-P. F.; Baker, T. A.; Cummins, C. C. *Organometallics* **2000**, *19*, 1622.
(31) Fryzuk, M. D.; Johnson, S. A.; Patrick, B. O.; Albinati, A.; Mason, S. A.; Koetzle, T. F. *J. Am. Chem. Soc.* **2001**, *123*, 3960.
(32) Studt, F.; MacKay, B.; Fryzuk, M. D.; Tuczek, F. *J. Am. Chem. Soc.* **2003**, *126*, 280.
(33) Studt, F.; Johnson, S. A.; MacKay, B.; Patrick, B. O.; Fryzuk, M. D.; Tuczek, F. *Chem.−Eur. J.* **2005**, *11*, 385.
(34) Fryzuk, M. D.; MacKay, B. A.; Johnson, S. A.; Patrick, B. O. *Angew. Chem., Int. Ed.* **2002**, *41*, 3709.
(35) MacKay, B.; Johnson, S. A.; Patrick, B. O.; Fryzuk, M. D. *Can. J. Chem.* **2005**, *83*, 315.
(36) MacKay, B. A.; Patrick, B. O.; Fryzuk, M. D. *Organometallics* **2005**, *24*, 3836.
(37) Fryzuk, M. D.; MacKay, B. A.; Patrick, B. O. *J. Am. Chem. Soc.* **2003**, *125*, 3234.

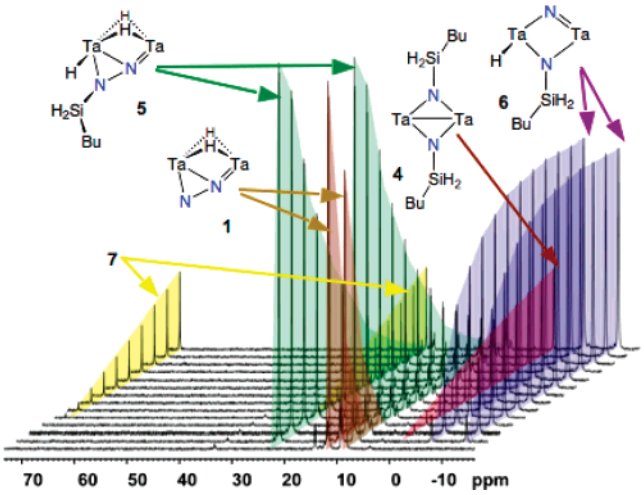

Figure 1. ^{31}P NMR spectra (hourly; lowest plot is time 0) showing species that arise in the reaction of **1** (brown) with an excess of butylsilane. The rapid appearance of **5** (green), its conversion to **6** (violet), and the appearance of **4** (red) and **7** (yellow) at the expense of **6** are evident. Conditions: 161 MHz (^{31}P), 300 K, C_6D_6 solution.

mechanism of the hydroalumination of **1** by conducting a series of consecutive timed ^{31}P NMR experiments using an internal standard for integration. Two intermediates, neither of which is persistent enough at room temperature for isolation or study using X-ray methods, were discovered using this technique.[36]

Figure 1 shows a stack plot of ^{31}P NMR experiments encompassing 13 h of the reaction between the starting dinitrogen complex **1** and 4 equiv of butylsilane. Resonances of **1** (brown) disappear rapidly at first, as resonances of the first intermediate **5** (green) arise. As communicated, the first intermediate **5** is then converted to a second intermediate, **6** (violet), and then conversion of this second intermediate **6** to the disilylimide **4** (red) is evident. As will be discussed later, when more than 2 equiv of butylsilane are used, a further transformation of **4** to **7** (yellow) can be detected.

Optimal conditions for isolation of the first intermediate **5** were developed by the addition of approximately 1 equiv of butylsilane to **1** and performing the reaction at −60 °C for 24 h; in this way, almost a quantitative yield of the monobutylsilylhydride **5** could be obtained in analytically pure form by precipitation from toluene using hexanes or pentane.

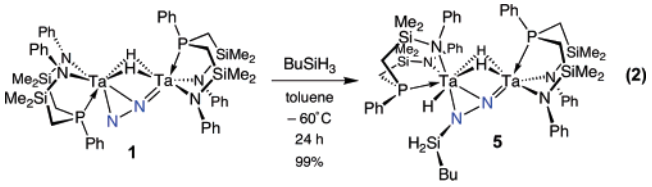

Although a discussion of the solid-state X-ray structure of **5** will not be reiterated here, it should be noted that **5** is nearly isostructural to the initial hydroboration addition product **2** and, from its solution data, very similar in structure to the corresponding hydroalumination adduct **3**, characterized by low-temperature NMR spectroscopy.[36] An intact N−N bond in these simple addition products is indicated by the ^{15}N NMR spectra of suitably labeled materials, in particular the presence of scalar coupling between the nitrogen nuclei of $^{1}J_{NN} = 16.6$ Hz for $^{15}N_2$−**5**.

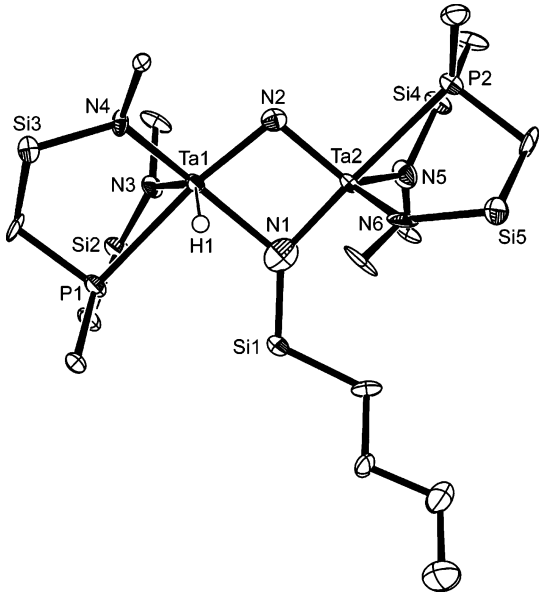

Figure 2. ORTEP drawing (ellipsoids at 50%) of the solid-state molecular structure of **6**. Silyl methyls and phenyl ring carbons other than ipso omitted for clarity. The hydride was modeled using XHYDEX.[38] Selected bond distances (Å), angles, and dihedral angles (deg): N1−N2 2.646(6); Ta1−Ta2 2.9258(6); Ta1−N2 1.928(11); Ta2−N2 1.874(9); Ta1−N1 2.187(10); Ta2−N1 1.924(10); N1−Si1 1.741(10); Ta1−P1 2.709(3); Ta1−N3 2.107(9); Ta1−N4 2.034(9); Ta2−P2 2.715(3); Ta2−N5 2.079(10); Ta2−N6 2.052(9); Ta1−N1−Si1 127.7(5); Ta2−N1−Si1 139.2(5); Ta1−N1−Ta1 90.5(4); Ta1−N2−Ta2 100.6(5); N1−Ta1−N2 80.0(4); N1−Ta2−N2 88.6(4); N2−Ta2−P2 94.1(3); N2−Ta1−P1 170.7(3); N3−Ta1−N4 100.3(4); N5−Ta2−N6 −118.0(4); N1−Ta1−Ta2−N2 174.0(6); P1−Ta1−Ta2−P2 −163.66(13).

That this first intermediate **5** is thermally unstable and rearranges to give the second intermediate **6** (eq 3) has already been communicated. Loss of H_2 from **5** provides the necessary additional electrons required to cleave the intact N−N bond, which leads to **6**. The ^{15}N NMR spectrum of **6** shows two resonances but no homonuclear scalar coupling, consistent with cleavage of the N−N bond. Since our original communication,[37] conditions have been developed to allow isolation of X-ray quality crystals of intermediate, **6**, thus allowing complete characterization of another mechanistically significant intermediate related to N−N bond cleavage in this system.

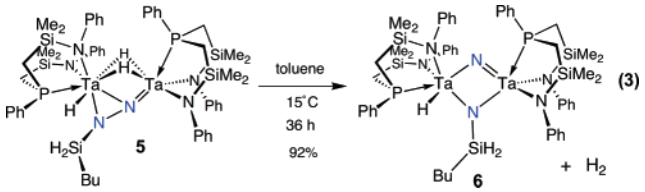

The solid-state molecular structure of **6** as determined by X-ray crystallography is shown in Figure 2, and it confirms our original assignment of this species as having separate bridging nitride and bridging silylimide units. The N1···N2 distance of 2.646(6) Å clearly indicates scission of the N−N bond in **6**. The absence of resonances consistent with bridging hydrides in the ^{1}H NMR spectrum of **6**, and the observation of free H_2 in ^{1}H NMR spectra recorded concurrently during the experiment illustrated in Figure 1, further supports our assertion that reductive cleavage of the N−N bond of the first intermediate **5** is linked to elimination of the bridging hydrides. In the solid state, the [NPN] ancillary ligands of **6** are arranged quasi trans to each other, which was also observed for complex **5**.

Scheme 1

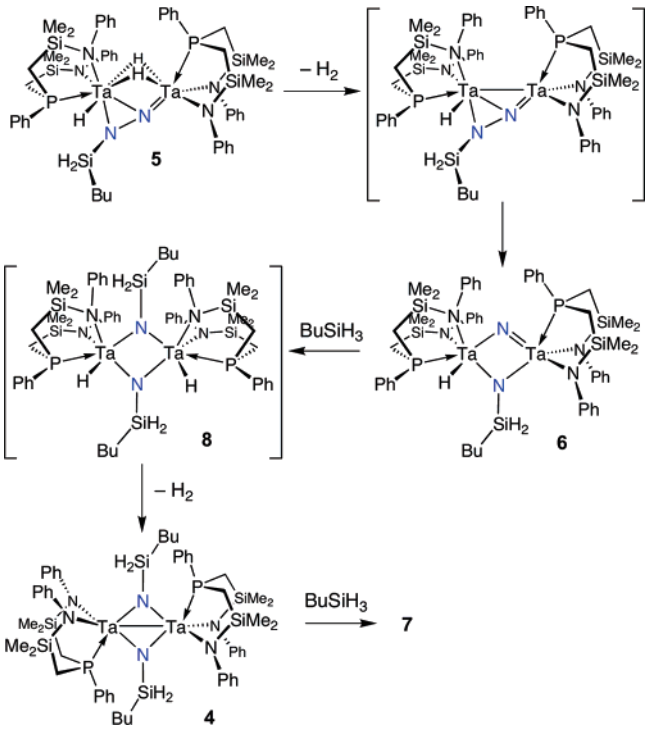

Bimetallic complexes featuring μ-nitrido ligands are rare, but the reported examples are dominated by group 5 complexes.[26,29,39,40] Mixed imido−nitrido derivatives featuring two metals are unprecedented[41] except for the ones that result from E−H addition to **1**. Examination of the Ta−N bond lengths in the complexes described herein are unremarkable when compared to other species with bridging nitrides in the literature.[42,43]

On the basis of the C_s symmetry apparent in the solution ^{1}H and ^{29}Si-DEPT NMR spectra of **6**, it appears that a fluxional process involving a "rocking" motion of the [NPN] ligand bound to Ta1, along with motion of hydride H1, occurs in solution. The atypical broadness (fwhm = 28 Hz) of the ^{31}P NMR resonances of **6** as compared to the sharp lines (fwhm = 2 to 4 Hz) observed for the other silylated derivatives may also be due to this process—the broadness persists in the spectrum of $^{15}N_2$−**6**, suggesting that this line width does not result from quadrupolar relaxation effects or coupling with ^{14}N nuclei.

Generation of the disilylimide product **4** from the second intermediate **6** requires the addition of a second equivalent of butylsilane across the bridging nitride to generate the additional μ-NSiH$_2$Bu unit and a new Ta−H, as shown in **8** below (Scheme 1). Although **8** is not observed by the monitoring experiment in Figure 1, loss of H_2 via a dinuclear reductive elimination would lead directly to **4**.

As reported elsewhere, DFT analysis of the conversion of the monobutylsilyl derivative **5** to the imide-nitride **6** has been carried out and confirms that the intermediate shown in Scheme 1 is computationally accessible.[44]

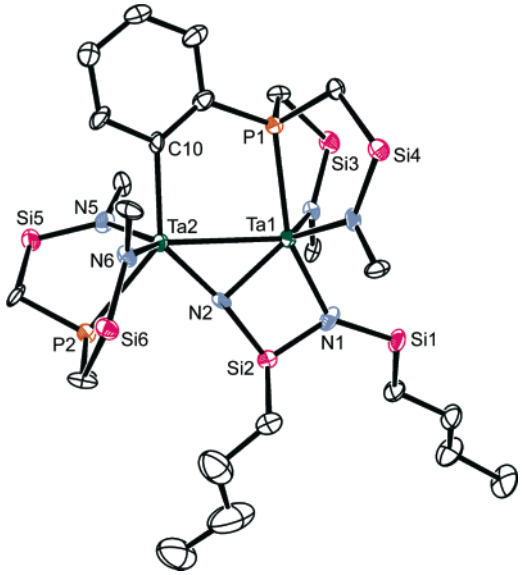

Figure 3. ORTEP drawing (ellipsoids at 50%) of the solid-state molecular structure of **7**. Silyl methyls and phenyl ring carbons other than ipso omitted for clarity. Selected bond distances (Å), angles, and dihedral angles (deg): N1−N2 2.549(6); Ta1−Ta2 2.9511(5); Ta1−N1 2.103(8); Ta1−N2 2.073-(7); Ta2−N2 1.972(8); N1−Si1 1.696(8); N1−Si2 1.703(9); N2−Si2 1.742-(8); Ta1−N3 2.065(7); Ta1−N4 2.078(8); Ta1−P1 2.597(2); Ta2−N5 2.085(8); Ta2−N6 2.095(7); Ta2−P2 2.637(2); Ta2−C10 2.276(9); Si1−N1−Si2 128.4(5); N1−Ta1−N2 75.2(3); N1−Si2−N2 95.4(4); Ta1−N2−Ta2 93.7(3); Ta2−Ta1−P1 83.59(5) Ta1−Ta2−P2 129.09(5); Ta1−Ta2−C10 92.3(2); N1−Ta1−Ta2−N2 4.1(4); N1−Ta1−Ta2−P2 9.2-(3); P1−Ta1−Ta2−C 106.3(2); P1−Ta1−Ta2−P2 −171.06(9); Si1−N1−Si2−N2 178.8(7).

A surprising finding from these sequential ^{31}P NMR experiments is the observation of additional peaks attributed to complex **7** (yellow-colored singlet resonances at δ 71.15 and 24.23 in Figure 1). This species was not observed in previous 2:1 reactions between butylsilane and dinitrogen complex **1**. The solid-state molecular structure obtained by X-ray diffraction (Figure 3) indicates that **7** involves a rearrangement of **4** accompanied by a final evolution of H_2, rather than a species resulting from further incorporation of free butylsilane into a derivative of **1**. The key differences between **7** and **4** are the ortho-metalation of one phenyl substituent of an [NPN] ligand phosphine donor by the opposite tantalum center, the eversion of one bridging silylimide to a new position, bridging Ta1 and Si2, and the formation of a new bond between Si2 and N1. Both dinitrogen-derived N atoms are still silylated, but they are no longer on opposite sides of the Ta···Ta internuclear axis.

^{1}H/^{29}Si HSQC NMR spectroscopy of **7** indicates one unique silyl hydride bound to Si2, keeping the coordination number of Si2 at four. In addition, two apparently equivalent silyl hydrides remain on Si1, consistent with the observed C_s symmetry of the molecule in solution.

Solutions of **1** in neat butylsilane form **7** as the major product when observed by ^{31}P NMR spectroscopy, implying that complex **7** is the endpoint of this reaction manifold. Interestingly, solutions of **4** are stable for weeks in the absence of excess butylsilane, even at elevated temperatures. The fact that the conversion of **4** to **7** requires additional BuSiH$_3$, which is not incorporated into the product, suggests a role for the silane;

(38) Orpen, A. G. *Dalton Trans.* **1980**, 2509.
(39) Berno, P.; Gambarotta, S. *Angew. Chem., Int. Ed. Engl.* **1995**, *34*, 822.
(40) Tayebani, M.; Feghali, K.; Gambarotta, S.; Bensimmon, C. *Organometallics* **1997**, *16*, 5084.
(41) Wigley, D. E. *Prog. Inorg. Chem.* **1994**, *42*, 239.
(42) Banaszak Holl, M. M.; Wolczanski, P. T.; van Duyne, G. D. *J. Am. Chem. Soc.* **1990**, *112*, 7989.
(43) Plenio, H.; Roesky, H. W.; noltmeyer, M.; Sheldrick, G. M. *Angew. Chem.* **1988**, *100*, 1377.
(44) Studt, F.; MacKay, B. A.; Fryzuk, M. D.; Tuczek, F. *Dalton Trans.* **2006**, 1137.

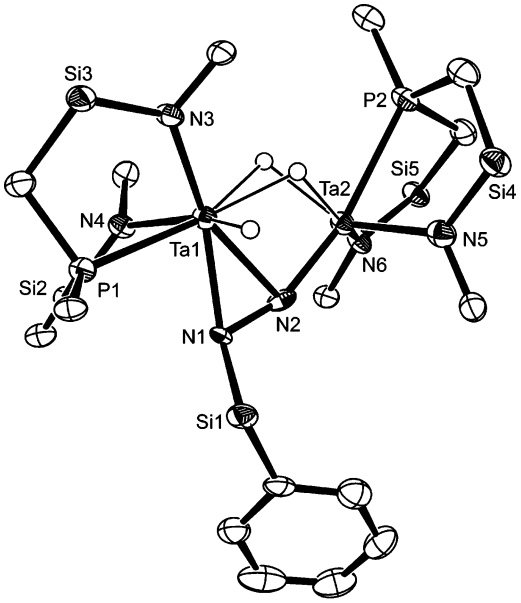

Figure 4. ORTEP drawing (ellipsoids at 50%) of the solid-state molecular structure of **9**. Silyl methyls and phenyl ring carbons other than ipso omitted for clarity. The hydrides were modeled using XHYDEX.[38] Selected bond distances (Å), angles, and dihedral angles (deg): N1−N2 1.354(10); Ta1−N 12.179(7); Ta1−Ta2 2.8393(14); Ta1−N2 2.214(6); Ta2−N2 1.860(8); N1−Si1 1.736(7); Ta1−N3 2.137(7); Ta1−N4 2.080(7); Ta1−P1 2.590-(2); Ta2−N5 2.049(7); Ta2−N6 2.041(8); Ta2−P2 2.635(3); Ta1−N1−Si1 135.2(4); Ta1−N1−N2 73.5(4); Ta1−N2−Ta2 87.9(3); N1−Ta1−P1 80.96(18); N1−Ta1−N3 161.7(3); N1−Ta1−N4 84.9(3); N2−Ta2−P2 167.6(2); N2−Ta2−N5 103.6(3); N2−Ta2−N6 108.7(5); N1−Ta1−Ta2−N2 −0.7(3); Ta2−Ta1−N1−Si1 106.9(5); P1−Ta1−Ta2−P2 −169.70-(14).

however, a mechanism for this process is not obvious. The net reaction is shown in eq 4.

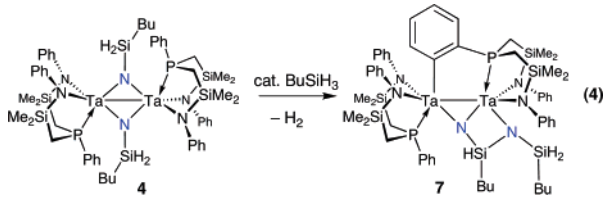

Hydrosilylation Using Phenylsilane ($PhSiH_3$). Phenylsilane reacts with the starting dinitrogen complex **1** in solution to give the expected phenylsilyl derivative, **9** (equation 5). The solution NMR spectral characteristics of **9** and its isotopologs are completely analogous to the already discussed butylsilyl complex **5**; the solid-state molecular structure of **9** (Figure 4) demonstrates that addition of phenylsilane to **1** results in a complex that is isostructural not only with **4** but also with the hydroboration adduct **2** previously reported.

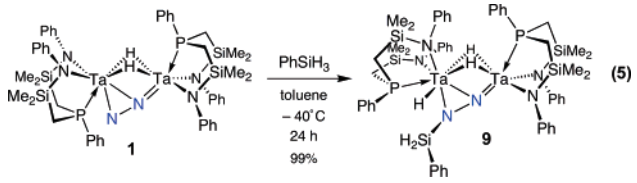

The solid-state metric parameters of the phenylsilane adduct **9** match those of the butylsilyl analogue **5**, within experimental error (3σ). The $^1J_{NN}$ coupling in $^{15}N_2$−**9** is 17.4 Hz, which is very near the value of 16.6 Hz reported for $^{15}N_2$−**5**. **9** shares

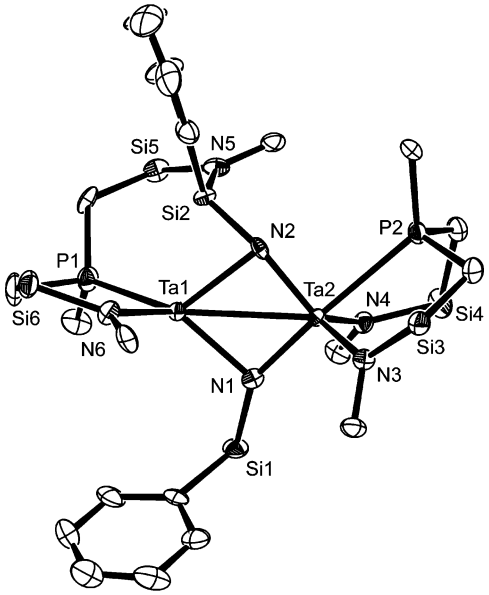

Figure 5. ORTEP drawing (ellipsoids at 50%) of the solid-state molecular structure of **11**. Silyl methyls and phenyl ring carbons other than ipso omitted for clarity. Selected bond distances (Å), angles, and dihedral angles (deg): N1−N2 2.827(3); Ta1−Ta2 2.9837(3); Ta2−N2 1.903(5); Ta2−N1 1.911-(5); Ta1−N2 2.253(5); Ta1−N1 2.158(4); N2−Si2 1.724(5); Si2−N5 1.758-(5); N1−Si1 1.729(5); Si2−Ta1 2.527(3); Ta2−N3 2.050(5); Ta2−N4 2.035(5); Ta2−P2 2.7962(17); Ta1−N6 2.032(5); Ta1−P1 2.5034(17); Ta1−N2−Ta2 91.4(2); Ta1−N1−Ta2 94.1(2); N1−Ta2−N2 95.17(19); N1−Ta1−N2 79.30(18); N2−Si2−N5 118.9(2); Ta2−Ta1−N6 127.08-(14); N3−Ta2−N4 114.61(19); N2−Ta2−P2 88.10(14); N6−Ta1−P1 82.47(15); Ta2−N1−Si1 146.1(3); N1−Ta1−N2−Ta2 177.9; P1−Ta1−Ta2−P2 73.31(10); Ta2−N2−Si2−N5 −108.9(2); N2−Ta2−N1−Si1 155.2(5).

the thermal instability common to this family of compounds, as it spontaneously converts to **10** in solution by the same method previously invoked for conversion of **5** to **6** (see eq 3). Although the solid-state molecular structure of **10** has not yet been established, its structure is likely closely related to **6** because of the similarity of their NMR spectra. For example, as for $^{15}N_2$−**6**, $^{15}N_2$−**10** shows no scalar coupling between the two resonances in its ^{15}N NMR spectrum, and the chemical shifts of the imido and nitrido atoms in these two homologues are similar. Furthermore, resonances typical of bridging hydrido ligands are absent in the ^{1}H NMR spectrum of **10**, and therefore, it seems that the silylation chemistries up to this point do not diverge when the silyl substituent changes.

However, in exploring this reaction manifold with sequential ^{31}P NMR experiments, it was found that a phenylsilyl analogue of the disilylimide **4** does *not* form. The imido nitrido complex **10** should be a substrate for a second hydrosilylation with phenylsilane, giving a symmetric structure in which both dinitrogen atoms are equivalently phenylsilylated, as in the conversion of **6** to **4** with butylsilane (Scheme 1). It is reasonable, therefore, to suggest that such a species should have a ^{31}P NMR chemical shift near 0 ppm as was observed for **4**. Instead, in the presence of additional equivalents of phenylsilane, **10** converts to a new complex **11**, which has a ^{31}P NMR spectrum consisting of two sharp singlets (δ −10.46 and +15.88) of equal intensity. The ^{1}H{^{31}P} and ^{29}Si−DEPT NMR spectra of this new species indicate C_1 solution symmetry—the latter shows six different silicon-29 resonances, four of which are typical of [NPN] ligand silyl groups with chemical shifts from δ 6 to 30 and $^2J_{PSi}$ values

Scheme 2

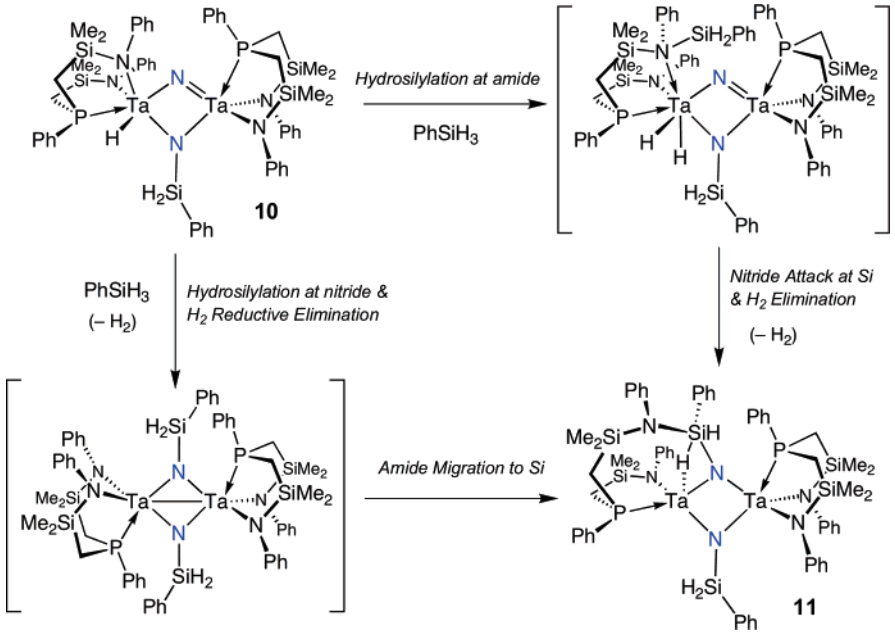

ranging from 0 to 20 Hz. Of the two remaining resonances, only one is typical of a silylimide (δ −35.82). The other occurs at δ 49.86 as a doublet (J_{PSi} = 41 Hz). The ^{15}N NMR spectrum of the appropriate enriched complex contains two resonances suggestive of silylimides; these resonances display no scalar coupling to each other. Fortunately, ochre crystals of **11** can be obtained from benzene solutions, and the solid-state molecular structure of **11** (Figure 5) reveals that an [NPN] ligand amide group has migrated from tantalum to silicon.

Silicon atom Si2 in Figure 5 is hypervalent—it is bound to a phenyl substituent, two N atoms, and two distinct hydrides as shown by the correlational ^{1}H/^{29}Si−DEPT NMR spectrum of **11**. The chemical shift of one of these hydrides is anomalously downfield (δ 9.43) for a silyl hydride. This resonance displays ^{29}Si satellites that indicate its $^{1}J_{SiH}$ coupling is 78.2 Hz, much less than the typical values of 114 to 168 Hz observed in other complexes in this study. These data and a small coupling to ^{31}P indicate that this hydride is likely shared between Si2 and Ta1, as shown in eq 8, although no artifacts indicating a hydride in a suitable position were resolvable in the difference map in the solid-state X-ray investigation. In retrospect, the ^{31}P NMR spectrum of **11** (both the chemical shift values and the absence of scalar J_{PP} coupling) is reminiscent of the final products of hydroalumination, which also feature [NPN] ligand amide migration (from Ta to Al). As for **6**, a Ta−Ta bond, resulting from elimination of two silane-derived hydrides as H_2 after the second hydrosilylation, is necessary to explain the observed diamagnetic behavior in **11**. Finally, the sequential ^{31}P NMR experiments described above show that **11** is the final complex to occur in the reactions of **1** with excess phenylsilane.

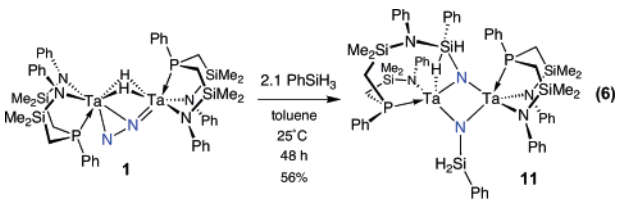

There is no suggestion of a similar [NPN] ligand amide migration in the chemistry of **1** with butylsilane. In fact, the conversion of **6** to **9** suggests that when butyl groups are present on the silyl addition reagent, the [NPN] ligand amides can remain bound to the tantalum atoms through extreme rearrangements of other portions of the molecule. The contrast between this finding and the amide migration observed in **11** indicates that silyl substituents play a role in organizing these complexes. Two mechanistic possibilities arise. In the first scenario, **11** results directly from amide migration in an intramolecular rearrangement of a complex that is isostructural with **4**. In the second scenario, the second equivalent of phenylsilane interacts with a ligand amide of **10** in an initial step and then with the bridging nitride to give **11**. This path implies poorer regioselectivity in the second hydrosilylation with phenylsilane versus butylsilane. These two alternatives are expressed in Scheme 2.

In the butylsilane manifold, it has already been shown that symmetrically functionalized complex **4** is available by direct hydrosilylation of the dinitrogen-derived bridging nitrido ligand of **6**. This suggested that complexes isostructural to **4** but incorporating two different substituents should be accessible. To demonstrate this, the synthesis of complex **12** was undertaken as shown in Scheme 3.

The ^{31}P NMR spectrum of **12** comprises a doublet of doublets (J_{PP} = 9.9 Hz), with both peaks very near the location of the single resonance observed for **4**. The ^{1}H and ^{29}Si NMR spectra both imply C_s symmetry for this molecule. **12** is also available from the complementary reaction between **10** and 1 equiv of butylsilane, suggesting that the order of addition (butyl vs phenyl) is unimportant (Scheme 3). This molecule is stable in solution, which implies that no amide migration is occurring (bottom of Scheme 2); this suggests that the second addition of $PhSiH_3$ to **10** leading to **11** probably proceeds at the ligand amido donor rather than at the bridging nitride. Therefore, the amide migration scenario in Scheme 2 is less likely in the formation of **11**, because it would appear that **12** does contain

Scheme 3

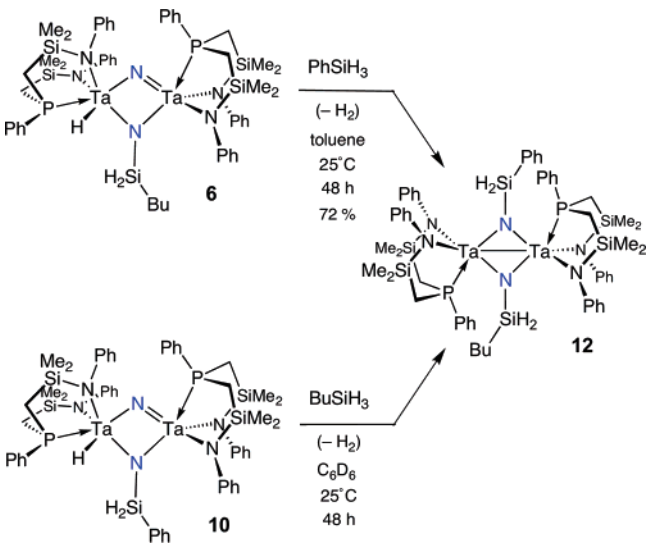

a bridging phenylsilyl imide and no migration occurs. This shows that a very subtle level of control over [NPN] ligand amide migration is at work, in that a small and perhaps remote difference in substituents can suppress rearrangement of ancillary ligands.

Hydrosilylation Using Ethanediylbissilane ($H_3SiCH_2CH_2SiH_3$). The ability to access dinuclear tantalum complexes with mixed silylimide functionality, such as **12** via the sequence in Scheme 3, suggested that two dinuclear complexes could be linked by the used of a bifunctional disilane. The idea was to examine the reaction of $H_3SiCH_2CH_2SiH_3$ with the isolable imide−nitride **6** in an 1:2 stoichiometry to isolate a tetranuclear complex of the formula $\{([NPN]Ta)_2(\mu\text{-}NSiH_2Bu)\}_2(\mu\text{-}NSiH_2\text{-}CH_2)_2$. The reaction proceeds at room temperature in toluene solution over a period of 4 days to generate a new complex characterized by a singlet in the ^{31}P NMR spectrum at δ −0.02 ppm. Isolation of crystalline material allowed determination of the solid-state molecular structure by X-ray crystallography (Figure 6). What is clearly evident is that the bifunctional silane has only added at one end to generate the disilylimide **13**, a closely related analogue of the original disilylimide **4**, which was formed by the addition of two equiv of $BuSiH_3$ to the starting dinitrogen complex **1**. This transformation is shown in eq 7.

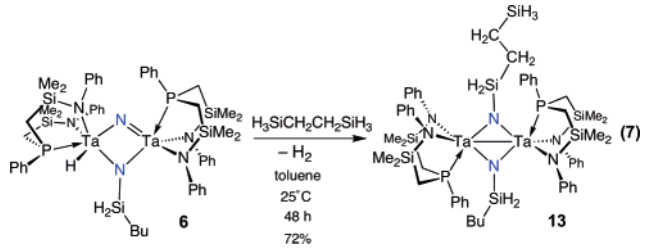

The $^{29}Si\{^1H\}$ NMR spectrum of isolated product **13** indicates the presence of three discrete alkylsilyl groups, which is consistent with the dinuclear formulation rather than the anticipated linked-tetranuclear target mentioned above. It is likely that the potentially reactive SiH_3 group that remains in **13** is not sterically available to other complexes with reactive Ta═N bonds because of the presence of the [NPN]-ligand phenyl groups.

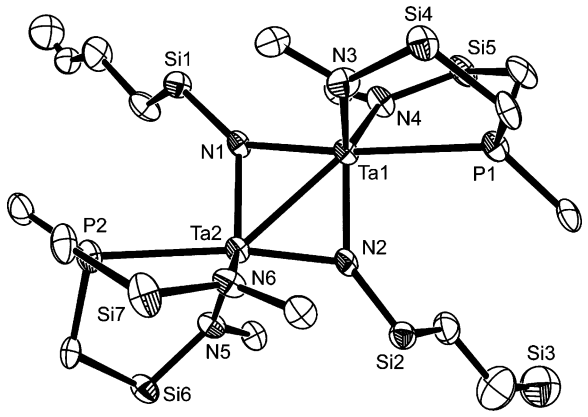

Figure 6. ORTEP drawing (ellipsoids at 50%) of the solid-state molecular structure of **13**. Silyl methyls and phenyl ring carbons other than ipso omitted for clarity. Selected bond distances (Å), angles, and dihedral angles (deg): N1···N2 2.979(4); Ta1−N1 2.022(7); Ta1−N2 2.031(7); Ta2−N1 2.013-(7); Ta2−N2 2.053(7); N1−Si1 1.710(8); N2−Si2 1.700(7); Ta1−Ta2 2.6759(5); Ta1−P1 2.744(2); Ta1−N3 2.076(7); Ta1−N4 2.083(7); Ta2−P2 2.688(2); Ta2−N5 2.092(7); Ta2−N6 2.078(7); Ta1−N1−Ta2 83.1(3); N1−Ta2−N2 94.3(3); Ta2−N2−Ta1 81.9(3); N2−Ta1−N1 74.7(3); Ta1−N1−Si1 142.4(4); Ta2−N2−Si2 136.2(4); Ta1−N2−Ta2−N1 −155.3(4); P1−Ta1−Ta2−P2 146.30(10).

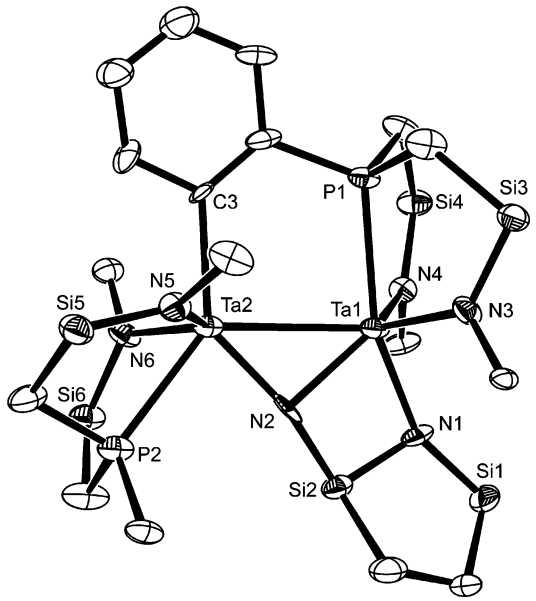

Figure 7. ORTEP drawing (ellipsoids at 50%) of the solid-state molecular structure of **14**. Silyl methyls and phenyl ring carbons other than ipso omitted for clarity. Selected bond distances (Å), angles, and dihedral angles (deg): N1−N2 2.609(6); Ta1−Ta2 2.9647(8); Ta1−N1 2.108(9); Ta1−N2 2.113-(9); Ta2−N2 1.944(12); N1−Si1 1.672(10); N1−Si2 1.757(11); N2−Si2 1.720(12); Ta1−N3 2.062(9); Ta1−N4 2.103(9); Ta1−P1 2.597(3); Ta2−N5 2.094(10); Ta2−N6 2.097(10); Ta2−P2 2.618(3); Ta2−C3 2.275-(10); Si1−N1−Si2 108.0(5); N1−Ta1−N2 76.3(4); N1−Si2−N2 97.2(4); Ta1−N2−Ta2 93.8(4); Ta2−Ta1−P1 83.40(7); Ta1−Ta2−P2 128.30(8); Ta1−Ta2−C3 92.3(3); N1−Ta1−Ta2−N2 −15.5(6); N1−Ta1−Ta2−P2 16.8(3); P1−Ta1−Ta2−C10 6.3(2); P1−Ta1−Ta2−P2 −9.2(3); Si1−N1−Si2−N2 166.6(6).

The availability of this bifunctional silylating agent also suggested that its chemistry with the starting dinitrogen complex **1** should be explored. Although the isolation of **13** suggests that linking multiple dinuclear tantalum complexes in an intermolecular fashion is unlikely, the possibility of an intramolecular disilylation was not initially precluded. The reaction between $H_3SiCH_2CH_2SiH_3$ and **1** in toluene proceeds initially as for butylsilane, forming complexes that are congeners of **5**

Scheme 4

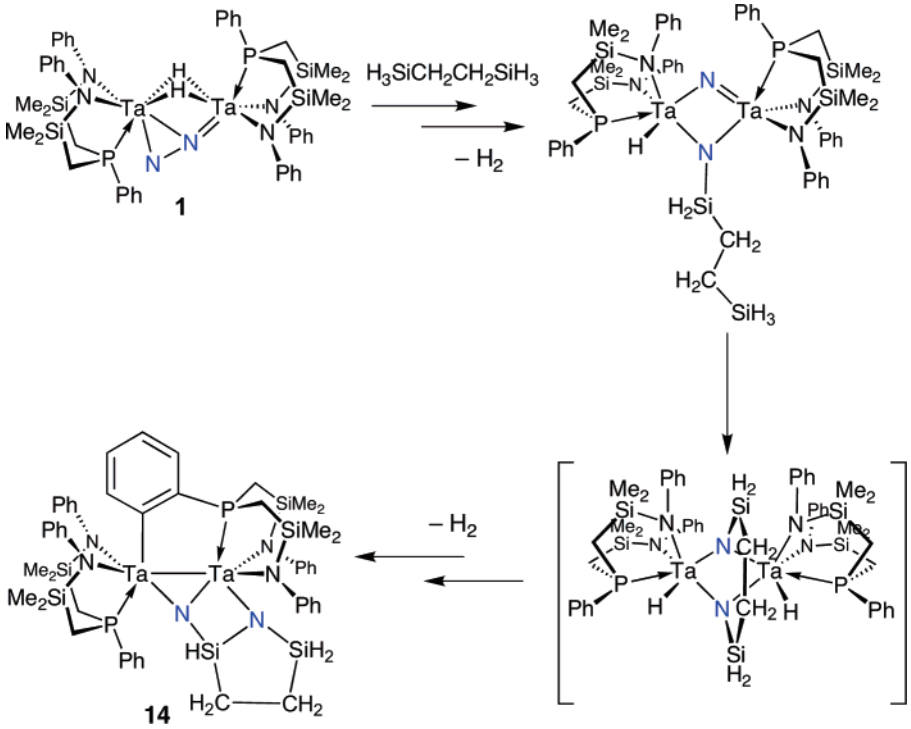

and **6** by their ^{31}P NMR spectra. On the basis of the spectral data for **4**, **12**, and **13**, resonances near 0 ppm would be expected for a second hydrosilylation, whether this second reaction were intramolecular or intermolecular. However, no such resonances were detected. Instead, resonances reminiscent of the cyclometalated complex **7** are observed; upon workup, the related complex **14** could be isolated as crystals. An ORTEP drawing of its solid-state molecular structure is shown in Figure 7. This complex exhibits the cyclometalation and imide displacement observed in **7**. The ^{1}H NMR spectra of the two species are similar, showing unique aryl resonances for the cyclometalated phenyl ring and apparent C_s molecular symmetry. As shown in Scheme 4, one possible explanation for the formation of this product is that the second silylation occurs intramolecularly but the strain of the ethanediyl bridge facilitates the eversion of the second imide nitrogen and promotes orthometalation of the phosphorus-phenyl. This is, of course, speculation.

Hydrosilylation Using Secondary Silanes. From the discussion above, it is clear that even within the primary silane manifold, a substituent change from butyl to phenyl at silicon affects rearrangements later in the hydrosilylation process. To probe this further, this reaction was extended to secondary silanes, in particulary diphenylsilane (Ph_2SiH_2) and methylphenylsilane ($MePhSiH_2$). Monitoring the reactions of each of these reagents with the starting dinitrogen complex **1** via ^{31}P NMR spectroscopy shows that only a transient amount of the hydrosilylated product homologous to **5** and **9** is ever observed; the decrease in the intensities of the resonances of **1** is matched by the appearance of resonances associated with complexes **15** ($R^1 = R^2 =$ Ph) and **16** ($R^1 =$ Me; $R^2 =$ Ph) as shown in eq 8. These reactions with either diphenylisilane or methylphenylsilane are very sluggish as compared to the reactions with butyl- and phenylsilane that generate **5** or **9**, respectively, which is likely due to steric effects and the decreased availability of reactive Si−H bonds in these reagents versus the primary silanes. Thus, the analogous first intermediates observed for primary silanes could not be isolated because they also possess the instability toward reductive elimination of H_2 coupled to N−N bond cleavage that is considered to be a hallmark of this type of complex. The rate at which this reaction occurs is not noticeably affected by the change from primary to secondary silanes, and therefore, conversion of the hydrosilylated complex to analogues of **6** and **10** is rapid as compared to hydrosilylation when secondary silanes are employed.

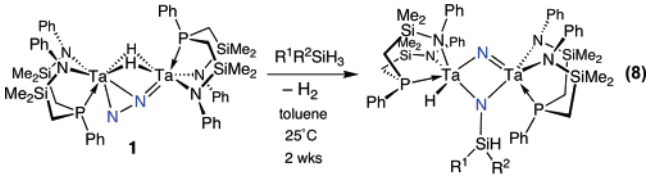

$R^1 = R^2 =$ Ph **15**

$R^1 =$ Me; $R^2 =$ Ph **16**

The imide−nitride complexes **15** (diphenylsilyl) and **16** (methylphenylsilyl) have been isolated, and the solid-state molecular structure of **16** is shown in Figure 8. In contrast to the primary silane homologues **6** and **10**, **16** features cis-disposed phosphines. Although this has not been observed elsewhere in the hydrosilylation chemistry, we have reported complexes resulting from hydroalumination[36] of **1** that also feature phosphines that are not as strictly trans oriented with respect to the Ta−Ta internuclear axis, as most derivatives of **1** appear to be.

The diphenylsilyl derivative **15** resembles the bridging nitrido complexes **6** and **10** by comparison of their ^{1}H and ^{31}P NMR spectra. The solid-state molecular structure of this complex has not yet been established. Although **15** and **16** should feature a reactive bridging nitride moiety, they do not react with additional equivalents of either primary or secondary silane. It is possible that the additional bulk of the secondary silane is compressing

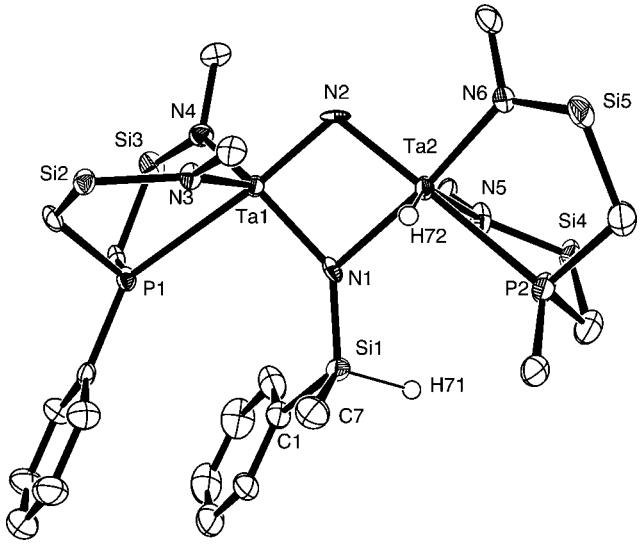

Figure 8. ORTEP drawing (ellipsoids at 50%) of the solid-state molecular structure of **16**. Silyl methyls and phenyl ring carbons other than ipso (will be) omitted for clarity. Selected bond distances (Å), angles, and dihedral angles (deg): Ta1−Ta2 2.914(3); Ta1−N3 2.040(5); Ta1−N1 1.961(6); Ta1−N4 2.055(5); Ta1−N_2 1.829(5); Ta1−P1 2.866(3); Ta2−N1 2.129(5); Ta2−N5 2.087(5); Ta2−N_2 1.960(6); Ta2−N6 2.093(6); N1−Si1 1.726(6); Ta2−P2 2.729(3); N1−Ta2−N5 95.2(2); Ta1−N1−Ta2 90.8(2); N1−Ta2−N6 165.4(2); N1−Ta2−N_2 −80.2(2); N1−Ta2−P2 99.95(16); Ta2−N2−Ta1 100.5(2); H101−Ta2−N5 142.5(3); N2−Ta1−N1 −88.1(2); N2−Ta1−N3 105.9(2); Ta1−N1−Si1 −140.1(3); N2−Ta1−N4 97.0(2); Ta2−N1−Si1 127.0(3); N2−Ta1−P1 169.31(16); N1−Ta1−N3 114.3(2); N1−Ta1−N4 129.8(2); N3−Ta1−N4 112.1(2).

the [NPN] ligand phenyl groups in a manner that prevents reactions at the bridging nitride position. In the particular case of **16**, it may be that cis-disposed phosphines negate further reactivity. In any case, the fundamental questions of how the silyl substituent affects the cascade of reactions experienced by derivatives of **1** remains unanswered. Resonances suggestive of complexes related to **4**, **7**, or **11** are not observed, even over weeks in the presence of butylsilane or phenylsilane. Although the lack of cyclometalation is significant, these complexes do not offer a cleaner route to homologues of **4** because they are unreactive.

Hydrosilylation Using Bulky Primary Silanes and Tertiary Silanes. A number of other simple silanes were examined for their ability to functionalize the starting dinitrogen complex **1**. Although mesitylsilane (2,4,6-$Me_3C_6H_2SiH_3$) reacts with **1**, there is no evidence for an addition product comparable to prototypical hydrosilylated complexes **5** and **9**. In fact, the ^{31}P NMR spectrum of the reaction mixture after 24 h contains a plethora of resonances, none of which could be tentatively identified as belonging to the family of complexes already described. This reaction was abandoned after several fruitless attempts at separating these compounds.

By contrast, *tert*-butylsilane (Me_3CSiH_3) appears to react with **1** via hydrosilylation as suggested by resonances comparable to those of **5** and **9** in the ^{31}P NMR spectra of 2:1 reactions. However, this material converts rapidly into other species. The lone isolated and fully characterized product features substantial degradation of ancillary ligands as well as N−N bond cleavage. It is presented in the Supporting Information rather than in the main text for brevity, as it offers little to this discussion other than to suggest once more that rearrangements of derivatives of **1** are governed by silyl substituents.

The reaction of the starting dinitrogen complex with tertiary silanes such as Me_3SiH does not proceed under any circumstances. Given the slow progress of the reaction with secondary silanes, it is likely that access to the coordinated N_2 unit is impeded by the bulkier tertiary silane.

Conclusions

The results of this study show that hydrosilylation of the dinitrogen complex **1** results in the formation of N−Si bonds and concomitant N−N bond cleavage. This process is comparable to the hydroboration and hydroalumination chemistries previously reported,[35,36] at least in the early stages. In particular, the first step in all of these processes is common and involves E−H addition across the Ta−N π-bond at the terminal nitrogen of the side-on end-on N_2 ligand, which initiates a series of steps that involves H_2 elimination and N−N bond cleavage. The hydrosilylation process discussed in this work has provided important details on these initial steps along with an understanding of what happens subsequently. The isolation and solid-state structural characterization of the key imide−nitride species **6** provides considerable insight into further functionalization of the bridging nitride of **6** by reaction with additional silane. For example, addition of butylsilane and subsequent elimination of H_2 result in the formation of the symmetrical disilylimide **4**; moreover, unsymmetrical disilylimide species such as **12** and **13** are also accessible due to isolation of intermediates such as **6** (and **10**).

One of the remarkable conclusions that arises from this work is how changes in the silane structure can affect the outcome of the reactions. Within the primary silane manifold, a change from butylsilane to phenylsilane changes the course of the addition of the second equivalent of silane, as evidenced by the isolation of the unsymmetrical product **11** in the reaction of $PhSiH_3$. How a remote substituent change can influence the mechanism is unknown, but one could speculate that transmission through the ancillary NPN ligands by some conformation change in the ligand binding could be responsible. Even more dramatic is the change in outcome when additional substituents are employed on the starting silane. For secondary silanes such as Ph_2SiH_2 and $MePhSiH_2$, the reaction slows down considerably and stops at the addition of one equivalent of silane as evidenced by the formation of the imide nitride derivatives **15** and **16**. The importance of steric effects in the silane structure is also apparent even with the primary silanes in that mesitylsilane is unreactive while *tert*-butylsilane undergoes more complicated transformations.

The initial observation that addition of two equiv of butylsilane to the dinitrogen complex **1** resulted in the formation of the symmetrical disilylimide species **4** suggested that perhaps additional silane might be able to further functionalize the nitrogen atoms and perhaps even release silylated amine. However, our attempts to accomplish this were thwarted by a intramolecular transformation rearrangement that involves cyclometalation of the P−Ph group across that $Ta_2(\mu\text{-}NSi)_2$ core, elimination of H_2, and rearrangement of the imide functionality. This process also was observed to occur for the reaction of ethanediylbissilane with **1**. The fact that this transformation requires additional silane to occur without the silane being incorporated has yet to be rationalized.

The transformations reported in this work, namely N−N bond cleavage and N−Si bond formation, hold promise for potential

discovery of homogeneous catalysts that can convert molecular nitrogen into higher value organonitrogen complexes. But there are still major hurdles to surmount. One avenue that we are exploring is iterative ancillary ligand design, which might mitigate some of the unproductive rearrangements reported herein.

Experimental Section

General Considerations. Unless otherwise stated, all manipulations were performed under an atmosphere of dry oxygen-free dinitrogen by means of standard Schlenk or glovebox techniques (Vacuum Atmospheres HE−553−2 glovebox equipped with a MO-40−2H purification system and a −60 °C freezer). Anhydrous hexanes and toluene were purchased from Aldrich, sparged with dinitrogen, and passed through columns containing activated alumina and Ridox catalyst before use. Anhydrous diethyl ether was stored over sieves and distilled from sodium benzophenone ketyl under argon. Pentane was stored over sieves and distilled from sodium benzophenone ketyl solublized by tetraglyme under dry dinitrogen prior to storage over a potassium mirror. Tetrahydrofuran was heated at reflux over CaH_2 prior to distillation from sodium benzophenone ketyl under argon. Nitrogen gas was dried and deoxygenated by passage through a column containing activated molecular sieves and MnO. The syntheses and characterization of compounds **4**, **5**, and **6** have been reported in our preliminary communication[34] along with the X-ray structures of **4** and **6** and details of their acquisition and solution; nevertheless, the Supporting Information for this manuscript has the preparations and spectral data reproduced for completeness.

Synthesis of [NP(C$_6$H$_4$)N]Ta(BuSiH$_2$N-μ-SiHBu-μ-N)Ta[NPN], 7. To a stirred solution of 235 mg (0.186 mmol) **1** in 15 mL toluene was added 65.5 mg (0.744 mmol, 4 equiv) of butylsilane in roughly 2 mL toluene under N_2. The dark-brown solution turned red initially and then dark brown over the course of 4 days. Solvent was removed under vacuum, leaving a brown residue that was triturated under hexanes. The resulting precipitate was recovered on a glass frit and rinsed with minimal hexanes to afford 112 mg (0.078 mmol, 42% yield) of **7**. In the assignment of the ^{1}H NMR spectrum, the protons on the metalated phenyl ring are labeled α, β, δ, and γ, with the proton nearest the metalated carbon labeled α. ^{1}H{^{31}P} NMR (C_7D_8, 30 °C, 400 MHz): δ −0.41, 0.11, 0.14, 0.29 (s, 6H each, SiCH_3), 0.68, 0.91, 1.31, 1.46 (d, 2H each, SiCH_2P), 3.37 (s, 2H, Si$_A$$H_2$), 4.62 (s, 1H, Si$_B$$H$), 0.49 (m, overlapping, 2H, Si$_A$CH_2CH$_2$−), 1.82 (br m, 2H, Si$_A$CH$_2$CH_2CH$_2$−), 1.04 (br, 2H, Si$_A$CH$_2$CH$_2$CH_2CH$_3$), 1.30, (d, 3H, Si$_A$CH$_2$CH$_2$CH$_2$CH_3), 0.13 (m, overlapping, 2H, Si$_B$CH_2CH$_2$−), 1.43 (br m, 2H, Si$_B$CH$_2$CH_2CH$_2$−), 1.78 (br, 2H, Si$_B$CH$_2$CH$_2$CH_2CH$_3$), 1.36, (d, 3H, Si$_B$CH$_2$CH$_2$CH$_2$CH_3), 7.61 (dd, 1H, H$_\alpha$), 7.21 (d, 1H, H$_\beta$), 7.21 (d, 1H, H$_\gamma$), 6.38 (d, 1H, H$_\delta$), 7.11, 7.72, 7.91 (P−C$_6$$H_5$) 6.89, 6.95, 7.05, 7.13, 7.20, 7.22 (d, t, 23H total, some overlap with solvent, N−C$_6$$H_5$). ^{31}P{^{1}H} NMR ($C_6D_6$, 30 °C, 161.97 MHz): δ 24.23 (s), 71.15 (s). Anal. Calcd for $C_{56}H_{82}N_6P_2Si_6Ta_2$: C 46.98; H 5.77; N 5.87. Found: C 47.12; H 5.91; N 5.89.

Synthesis of $^{15}N_2$−7. A solution of $^{15}N_2$−**1** was treated in a manner similar to the preparation of **7**. ^{31}P{^{1}H} NMR (C_6D_6, 30 °C, 161.97 MHz): δ 24.23 (s), 71.15 (d, $^2J_{PN}$ = 9.9 Hz). ^{15}N NMR (C_6D_6, 30 °C, 40 MHz) δ −17.5 (d, $^2J_{PN}$ = 9.9 Hz), 233.4 (s).

^{31}P NMR Spectroscopic Investigation of the Reaction of 1 with Butylsilane or Phenylsilane. A 9" Wilmad NMR tube was charged with ∼40 mg **1** in roughly 0.8 mL C_6D_6 and a sealed glass capillary tube containing neat P(OMe)$_3$ as an internal reference. The tube was sealed with a 5 mm rubber septum and wrapped with ParaFilm laboratory film and inserted into the probe of a Bruker AVA-400 NMR spectrometer. The spectrometer was programmed to observe consecutive sets of ^{1}H{^{31}P} and ^{31}P{^{1}H} spectra every 15 min for 25 h. After initial spectrometer calibration was performed, the sample was ejected and 14 mg neat butylsilane (roughly 4.5 equivs) or a comparable amount of a solution of phenylsilane in approximately 0.25 mL C_6D_6 was added as a bolus through the septum using a 20-gauge hypodermic needle. The reagents were mixed by brief inversion of the tube before the sample was returned to the probe and automated acquisition was begun. Individual resonances were integrated with respect to the internal standard. Similar experiments using D_2−**1** and $^{15}N_2$−**1** were also conducted.

Synthesis of ([NPN]TaH)(μ-H)$_2$(μ-η^1:η^2-NNSiH$_2$Ph)(Ta[NPN]), 9. To a stirred solution of 441 mg (0.350 mmol) **1** in 25 mL toluene was added 37.9 mg (0.35 mmol, 1 equiv) of phenylsilane in roughly 2 mL toluene under N_2. The flask was stored for 24 h in a freezer, after which the dark-brown solution had turned red-orange. Solvent was removed under vacuum, leaving a pink residue that was triturated under hexanes and left overnight. The resulting red crystalline material was recovered on a glass frit, yielding 488 mg (0.345 mmol, 99% yield) **9**. Cocrystallized hexanes (0.5 equiv) could not be removed from the solid under full vacuum, and its presence was confirmed by NMR and X-ray crystallography. ^{1}H NMR (C_7D_8, −60 °C, 400 MHz): δ −0.12, −0.07, −0.02, 0.01, 0.02, 0.05, 0.09, 0.52 (s, 3H each, total 24 SiCH_3), 0.47, 0.81, 1.25, 1.29, 1.37, 1.58, 1.74, and 1.89 (AMX, 1H each, SiCH_2P), 4.62 and 5.38 (d, $^2J_{HH}$ 10.9 Hz, 1H each, NSiH_2Ph), 6.76, (*o*-C$_6$$H_5$−Si), 6.82, 7.11 (C$_6$$H_5$−Si), 7.38 (d, J_{HH} = 7.3, *o*-C$_6$$H_5$−P) 8.40 (d, J_{HH} = 5.0, *o*-C$_6$$H_5$−P) 6.47, 6.76, 6.82, 6.95, 7.13, 7.18, 7.20, 7.28, 7.46 (overlapping m, PPh−*H* and NPh−*H*), 11.24 (ddd, 2H, J_{HH} = 10.1 and 5.24 Hz, J_{HP} = 22.1 Hz, Ta*H*Ta) 14.30 (dd, $^2J_{HP}$ = 18.1 Hz, J_{HH} = 5.24 Hz, 1H, Ta−H$_t$).^{13}C NMR (C_7D_8, −60 °C, 100.61 MHz): −0.33, 0.52, 0.80, 0.97, 2.19, 2.86, 3.85, 4.14 (s, Si*C*H$_3$), 15.06, 15.39, 16.24, 17.18, 22.32, 22.05, 19.58, 20.69 (d, Si*C*H$_2$P), 130.02 (*o*-*C*$_6$H$_5$−Si) 132.03 and 133.60 (*o*-*C*$_6$H$_5$−P) 116.44, 117.86, 121.87, 122.46, 123.01, 126.31, 129.22, 130.02, 132.65, 1334.16, 136.31, 138.44, 139.89, 143.98, 145.77, 146.21, 147.04, 147.69, 152.37, 155.69, 156.81, 157.31 (P(*C*$_6$H$_5$) and N(*C*$_6$H$_5$). ^{31}P{^{1}H} NMR (C_7D_8, −60 °C, 161.97 MHz): δ 23.27 (d, J_{PP} = 17.8 Hz), 8.86 (d, J_{PP} = 17.8 Hz). ^{29}Si NMR (C_7D_8, −60 °C, 79.5 MHz) δ −9.26 (s, NS*i*H$_2$Ph) 6.73 (d, $^2J_{PSi}$ = 9.6 Hz), 7.16 (d, $^2J_{PSi}$ = 9.6 Hz) 10.68 (d, $^2J_{PSi}$ = 11.3 Hz), 11.30 (d, $^2J_{PSi}$ = 9.6 Hz). UV−Vis: λ_{max} = 500 nm, ϵ = 619 M^{-1} cm^{-1}. Anal. Calcd for $C_{54}H_{72}N_6P_2Si_5Ta_2\cdot(C_6H_{14})_{0.5}$ C 48.47; H 5.64; N 5.95. Found: C 48.63; H 5.20; N 5.48.

Synthesis of $^{15}N_2$−9. A solution of $^{15}N_2$−**1** was treated in a manner similar to the preparation of **9**. ^{15}N NMR (C_7D_8, −60 °C, 40 MHz) δ −139.7 (d, $^1J_{NN}$ = 17.4 Hz) −50.5 (dd, $^2J_{PN}$ = 26.1 Hz, $^1J_{NN}$ = 17.4 Hz). Additional coupling of 26.1 Hz was observed in the δ 23.27 ppm resonance in the ^{31}P{^{1}H} spectrum, as was an additional coupling of 4.9 Hz in the δ −9.26 ppm resonance of the ^{29}Si{^{1}H} spectrum.

Synthesis of ([NPN]TaH)(μ-N)(μ-NSiH$_2$Ph)(Ta[NPN]), 10. A red-orange 25 mL toluene solution of **9** (488 mg, 0.345 mmol) was left at 15 °C under N_2 for 36 h, after which the solvent was removed under vacuum, leaving a yellow-brown residue, which was triturated under hexanes. Solid powdery **10** was recovered on a glass frit and rinsed with hot hexanes to remove a brown impurity (473 mg, 0.335 mmol, 97% yield). ^{1}H NMR (C_6D_6, 30 °C, 400 MHz): δ −0.18, −0.04, 0.03 and 0.41 (s, 6H each, 24H total, SiCH_3), 0.98, 1.16, 1.34, and 1.48 (d, 2H each, SiCH_2P), 4.76 (b, 2H, NSiH_2Ph), 6.48, 6.92, 7.08, 7.47, 6.94, 7.09, 7.15, 7.38, and 7.61 (overlapping m, PPh−*H* and NPh−*H*) 7.92 and 7.41 (m, 2H each, PPh-*o*-*H*), 18.21 (d, $^2J_{HP}$ = 47.3 Hz, 1H, Ta−H$_t$). ^{31}P{^{1}H} NMR (C_6D_6, 30 °C, 161.97 MHz): δ −5.4 (b), −12.8 (b). ^{29}Si NMR (C_6D_6, 30 °C, 79.5 MHz) δ −38.62 (s, NS*i*H$_2$Ph) 11.51 (d, $^2J_{PSi}$ = 12.1 Hz), 10.81 (d, $^2J_{PSi}$ = 12.4 Hz). Anal. Calcd for $C_{54}H_{70}N_6P_2Si_5Ta_2$: C 47.43; H 5.16; N 6.15. Found: C 47.80; H 5.51; N 5.94.

Synthesis of $^{15}N_2$−10. A solution of $^{15}N_2$−**9** in C_6D_6 was allowed to decompose overnight at room temperature. ^{15}N NMR (C_6D_6, 30 °C, 40 MHz) δ 312.2 (b) −36.9 (d, $^2J_{PN}$ = 17.2 Hz,). Additional coupling of 17.2 Hz was observed in the δ −12.8 ppm resonance in the ^{31}P{^{1}H} spectrum, as was an additional coupling of 4.1 Hz in the δ −38.6 ppm resonance of the ^{29}Si{^{1}H} spectrum.

Synthesis of ([NPN]Ta)(μ-NSiH$_2$Ph)(μ-NSiHPh)(Ta[NPN]), 11. To a stirred solution of 312 mg (0.247 mmol) **1** in 15 mL toluene was added 55.0 mg (0.510 mmol, 2.1 equiv) of phenylsilane in roughly 2 mL toluene under N_2. The dark-brown solution turned dark red over the course of 48 h, and the solvent was removed under vacuum, leaving a brown residue, which was triturated under hexanes. An ochre precipitate was recovered on a glass frit, giving 205 mg (0.139 mmol, 56% yield) of analytically pure **11**. ^{1}H{^{31}P} NMR (C_6D_6, 30 °C, 400 MHz): δ −0.39, −0.24, −0.23, −0.19, −0.13, −0.01, 0.22, 0.59 (s, 3H each, SiCH_3), 1.13, 1.23, 1.28, 1.43, 1.61, 1.94, 2.29, and 2.79 ppm (AMX, 1H each, SiCH_2P), 4.60 and 5.68 (d, 1H each, $^2J_{HH}$ = 13.3 Hz, PhSiH_2−N), 5.59 (s, N−PhSi(H)−N), 7.54, 7.62 (d, 2H each, o-C_6H_5−P) 9.43 (s, 2H o-C_6H_5−SiH_2−N), 6.52, 6.69, 6.79, 6.88, 6.93, 7.04, 7.21, 7.36, 8.18 (overlapping m, PPh−H and NPh−H). ^{13}C NMR (C_6D_6, 30 °C, 100.61 MHz): δ −1.56, −0.59, −0.38, 0.87, 3.30, 4.03, 4.12, 4.81 (SiCH_3), 15.22, 18.14, 24.22, 35.17 (CH_2−P), 125.91 (N-o-C_6H_5Si(H)−N) 129.07 (o−C_6H_5−SiH_2−N), 123.47, 124.44, 126.39, 127.85, 129.58, 132.48, 133.69, 137.58 (P−C_6H_5 and N−C_6H_5). ^{31}P{^{1}H} NMR (C_6D_6, 30 °C, 161.97 MHz): δ −10.46, 15.88 ppm (s). ^{29}Si NMR (C_6D_6, 30 °C, 79.5 MHz) δ −35.82, (dd, $^2J_{PSi}$ = 12.2, 16.6 Hz, N−PhSi(H)−N) 6.07 (s, [NPN] ligand) 12.93 (d, $^2J_{PSi}$ = 14.8 Hz, [NPN] ligand), 17.07 (d, $^2J_{PSi}$ = 14.8 Hz, [NPN] ligand), 18.30 (d, $^2J_{PSi}$ = 20.1 Hz, [NPN] ligand), 49.86 (d, $^2J_{PSi}$ = 41.0 Hz, PhSiH_2−N). Anal. Calcd for $C_{60}H_{74}N_6P_2Si_6Ta_2$: C 48.90; H 5.20; N 5.70. Found: C 48.63; H 5.20; N 5.48.

Synthesis of $^{15}N_2$−11. A solution of $^{15}N_2$−**1** was treated in a manner similar to the preparation of **11**. ^{31}P{^{1}H} NMR (C_6D_6, 30 °C, 161.97 MHz): δ −10.46 (d, J_{PN} = 17.86 Hz), 15.88 ppm (s). ^{15}N NMR (C_6D_6, 30 °C, 40 MHz) δ −61.21 (d, J_{PN} = 17.86 Hz), −35.84 (s). ^{29}Si NMR (C_6D_6, 30 °C, 79.5 MHz) δ −35.82, (ddd, $^2J_{PSi}$ = 12.2, 16.6 Hz, $^1J_{NSi}$ = 10.5 Hz, N−PhSi(H)−N), 49.86 (dd, $^2J_{PSi}$ = 41.0 Hz, PhSiH_2−N), [NPN] ligand silyl resonances unaffected.

Synthesis of ([NPN]Ta)$_2$(μ-NSiH$_2$Bu)(μ-NSiH$_2$Ph), 12. To a stirred 20 mL toluene solution of 126 mg (0.094 mmol, ∼1 equiv) **6** was added 9 mg (0.10 mmol) phenylsilane. The stirred solution turned deep red over 2 days. The solvent was evaporated, and the dark solids were triturated under pentane, giving 97.8 mg **12** (0.067 mmol, 72% yield). Alternately, **10** was combined with butylsilane in C_6D_6 in an NMR tube, and the ^{31}P NMR resonances of **12** were observed after 2 days. No yield is reported in the absence of an internal standard. ^{1}H-{^{31}P} NMR (C_6D_6, 30 °C, 400 MHz): δ −0.14, −0.12, 0.02, 0.10, (s, 6H each, SiCH_3), −0.31 (br, 2H, SiCH_2CH$_2$−), 0.62 (br m, 2H, −CH$_2$CH_2CH$_2$−), 1.24 (br, 2H, −CH$_2$CH_2CH$_3$), 0.856 (d, 3H, CH$_2$CH_3), 1.02, 1.16, 1.31, and 1.64 ppm (d, 2H each, SiCH_2P), 4.78 (s, 2H, PhSiH_2−N), 4.41 (s, 2H BuSiH_2−N), 6.37 (d, 2H, o-C_6H_5−Si), 7.34 and 7.49 (d, 2H each, o-C_6H_5−Si) 4.91 (s, 2H, SiH_2) 6.941 (d, 4H, p-HPhN), 7.11 (dd, 8H, m-HPhN), 6.52 (d, 8H, m-HPhN), 7.12 (d, 2H, p−HPhP), 7.20 (dd, 4H, m−HPhP) and 7.65 (d, 2H, o−HPhP), 6.87, 6.93, 6.95, 6.97, 6.99, 7.05, 7.08, 7.23, 7.27 (overlapping m, PPh−H and NPh−H). ^{31}P{^{1}H} NMR (C_6D_6, 30 °C, 161.97 MHz): δ −1.17 ppm (d, J_{PP} = 9.9 Hz), −0.70 (d, J_{PP} = 9.9 Hz). ^{29}Si NMR (C_6D_6, 30 °C, 79.5 MHz) δ −11.3, (d, $^2J_{PSi}$ = 8.0 Hz, PhSiH_2−N), −1.8 (d, $^2J_{PSi}$ = 8.8 Hz, BuSiH_2−N), 10.93 (d, $^2J_{PSi}$ = 14.8 Hz, [NPN] ligand) 12.9 (d, $^2J_{PSi}$ = 12.4 Hz [NPN] ligand) Anal. Calcd for $C_{58}H_{80}N_6P_2Si_6Ta_2$: C 47.92; H 5.55; N 5.78. Found: C 47.60; H 5.15; N 6.07.

Synthesis of ([NPN]Ta)$_2$(μ-NSiH$_2$Bu)(μ-NSiH$_2$CH$_2$CH$_2$SiH$_3$), 13. To a stirred 15 mL toluene solution of 383 mg (0.284 mmol, 1 equiv) **6** was added 25.7 mg (0.284 mmol) ethanediylbissilane. The stirred solution turned deep red over 4 days. The solvent was evaporated, and the dark solids were triturated under pentane, giving 289 mg **13** (0.202 mmol, 71% yield). ^{1}H{^{31}P} NMR (C_6D_6, 30 °C, 400 MHz): δ 0.00, 0.11, 0.38, 0.40, (s, 6H each, SiCH_3), −0.35 (br, 2H, SiCH_2CH$_2$−), −0.12 (br m, 2H, −CH$_2$CH_2CH$_2$−), 1.58 (br, 2H, −CH$_2$CH_2CH$_3$), 1.02 (d, 3H, CH$_2$CH_3), −0.05 (d, 2H, N−SiH$_2$CH$_2$CH_2-SiH$_3$), 0.34 (d, 2H, N−SiH$_2$CH_2CH$_2$SiH$_3$) 1.63 ppm (AMX, 8H, SiCH_2P), 3.63 (t, $^2J_{HH}$ = 3.8 Hz, 3H, H_3CSiEtSiH$_2$−N), 4.81 (d, $^2J_{HH}$ = 3.56 Hz, H$_3$CSiEtSiH_2−N), 4.89 (s, 2H, SiH_2Bu), 7.62 (d, 4H, o-HPhP), 6.90, 6.92, 7.01, 7.06, 7.10, 7.12, 7.19, 7.22 (overlapping m, PPh−H and NPh−H). ^{13}C NMR (C_6D_6, 30 °C, 100.61 MHz): δ −2.42, 1.52, 4.85, 5.12 (SiCH_3), 25.11, 26.20 (CH_2−P) 25.11, 26.20, 13.96, 3.87 (BuSiH_2), 3.87 (H$_3$SiCH_2), 12.89 (H$_3$SiCH$_2$CH_2SiH$_2$−N), 131.46, 131.57 (o-Ph−P), 122.44, 122.54, 123.61, 125.21, 128.10, 128.50, 128.66, 128.84 (PPh and NPh). ^{31}P{^{1}H} NMR (C_6D_6, 30 °C, 161.97 MHz): δ −0.021 ppm (m). ^{29}Si−DEPT NMR (C_6D_6, 30 °C, 79.5 MHz) δ −2.14 (H$_3$SiEtSiH$_2$−N), −0.01 (BuSiH$_2$−N) 8.08 (d, $^2J_{PSi}$ = 15.7 Hz, [NPN] ligand) 8.79 (d, $^2J_{PSi}$ = 17.4 Hz, [NPN] ligand). H$_3Si$−Et silyl resonance not located. Anal. Calcd for $C_{54}H_{82}N_6P_2Si_7Ta_2$: C 45.18; H 5.76; N 5.85. Found: C 45.23; H 5.91; N 5.96.

Synthesis of [NP(C$_6$H$_4$)N]Ta(NSiH$_2$CH$_2$CH$_2$Si(H)-μ-N)Ta[NPN], 14. To a stirred 10 mL toluene solution of 184 mg (146 mmol) **1** was added neat ethanediylbissilane (13 mg, 146 mmol, 1 equiv). The solution was allowed to sit overnight, and solvent was removed under vacuum to give a yellow-brown residue that yielded crystalline **14** (138 mg, 105 mmol, 72% yield) after trituration under hexanes and 24 h at −60 °C in a glovebox freezer.^{1}H{^{31}P} NMR (C_7D_8, 30 °C, 400 MHz): δ −0.80, −0.08, 0.13, 0.47 (s, 6H each, 24H total, SiCH_3), 0.68, 0.92, 1.34, 1.76 (d, 2H each, −CH_2P), 3.52 (s, 2H, SiH_2), 4.11 (s, 1H, SiH) 7.74 (d, 2H, o-C_6H_5−P), 7.72 (dd, 1H, H$_\alpha$), 7.03 (d, 1H, H$_\beta$), 6.47 (d, 1H, H$_\gamma$), 6.79 (d, 1H, H$_\delta$) 6.82, 6.84, 6.91, 7.02, 7.14, 7.31, 7.44 (d, t, overlapping with solvent resonances, C_6H_5−N and C_6H_5−Ph). ^{31}P{^{1}H} NMR (C_7D_8, 30 °C, 400 MHz): δ 21.7 (s), 72.8 (s). Elemental analysis was not obtained.

Synthesis of ([NPN]TaH)(μ-N)(μ-NSiHPh$_2$)(Ta[NPN]), 15. To a 15 mL toluene solution of 268 mg (212 mmol) **1** was added 39.3 mg (213 mmol, ∼1 equiv) Ph$_2$SiH$_2$ in roughly 2 mL toluene. The mixture was agitated briefly and allowed to stand under N_2 at ambient temperature. The ^{31}P NMR spectrum of a portion of the solution withdrawn after 2 weeks indicated conversion to a new product, and solvent was removed under vacuum. Brown residues were triturated under hexanes and 191 mg (131 mmol, 62% yield) of yellow-white powdery **15** were isolated on a frit after rinsing with minimal hexanes. ^{1}H{^{31}P} NMR (C_7D_8, 30 °C, 400 MHz): δ −0.28, −0.03, 0.16, 0.31 (s, 6H each, 24H total, SiCH_3), 0.84, 0.92, 1.36, 1.49 (d, 2H each, −CH_2P), 3.49 (s, 1H, SiH) 7.83, 7.90 (d, 2H each, o-C_6H_5−P), 6.85, 6.92, 7.14, 7.33, 7.38, 7.41 (d, t, overlapping with solvent resonances, C_6H_5−N and C_6H_5−Ph), 6.43, 7.11, 7.34 (d, t, 10H total, C_6H_5Si). ^{31}P{^{1}H} NMR (C_7D_8, 30 °C, 400 MHz): δ − 16.54 (vb, fwhm 36.2 Hz). −9.47 (vb, fwhm 36.8 Hz). Anal. Calcd for $C_{60}H_{84}N_6P_2Si_5Ta_2$: C 49.58; H 5.82; N 5.78. Found: C 49.33; H 5.91; N 5.86.

([NPN]TaH)(μ-N)(μ-NSiH(Me)Ph)(Ta[NPN]), 16. To a dark brown solution of **1** (0.20 g, 0.16 mmol) in 5 mL of toluene was added 0.019 g of methylphenylsilane under N_2. Over the course of 4 days, the solution turned red. The solvent was removed under vacuum, and the resulting red solid was dissolved in hexanes. Yellowish-red crystals were obtained (0.080 g, 37%) over a course of 48 h at room temperature and were collected in a glass frit and rinsed with pentane. A pentane solution of **16** was cooled to −30 °C, and single crystals suitable for X-ray analysis were obtained. ^{1}H NMR (C_7D_8, −70 °C, 500 MHz): δ(ppm) −0.15, −0.09, −0.02, 0.08, 0.13, 0.28, 0.33, 0.40, 0.44 (overlapping s, 24H total, SiCH_3), 0.99, 1.06, 1.17, 1.29, 1.45, 1.54, 1.64, 1.74 (overlapping, 11H total, SiCH_2P and NSiCH_3), 4.58, 4.88, 5.24, 5.32 (s, 1H total, NSiH), 6.0 to 8.1 (overlapping, SiPh−H, PPh−H and NPh−H), 16.79, 16.86, 16.95, 17.44, 17.51 17.65 (overlapping m, 1H total, Ta−H$_t$). ^{31}P{^{1}H} NMR (C_7D_8, −70 °C, 500 MHz) δ(ppm) 1.64, −4.70, −11.03, 11.70, −15.78, −16.92, −21.35. ^{31}P COSY correlation between δ(ppm) −1.64 and −16.92, −11.03 and −21.35, −15.39 and −15.78. Anal. Calcd for $C_{55}H_{71}N_6P_2Si_5Ta_2$: C, 47.82; H, 5.25; N, 6.08. Found: C, 47.92; H, 5.58; N, 6.19

Acknowledgment. We are grateful to NSERC of Canada for funding (Discovery Grant for M.D.F., PGS-A and PGS-B to B.A.M.) and to Dr. Christopher D. Carmichael for his assistance with the diffraction experiments.

Supporting Information Available: Full experimental details for the synthesis of complexes **4**, **5**, and **6**; experimental details for the X-ray crystal structure analyses; CIF files for complexes **6**, **7**, **9**, **11**, **13**, **14**, and **16**; experimental details for the reaction of $^{t}BuSiH_3$ with the dinitrogen complex **1**. This material is available free of charge via the Internet at http://acs.pubs.org.

JA061508Q